Massive symmetry breaking in $LaAlO_3/SrTiO_3(111)$ quantum wells: a three-orbital, strongly correlated generalization of graphene

David Doennig,[1] Warren E. Pickett,[2] and Rossitza Pentcheva[1,*]

[1]*Department of Earth and Environmental Sciences, Section Crystallography and Center of Nanoscience, University of Munich, Theresienstr. 41, 80333 Munich, Germany*

[2]*Department of Physics, University of California Davis, One Shields Avenue, Davis, CA 95616, U.S.A.*

(Dated: March 29, 2013)

Density functional theory calculations with an on-site Coulomb repulsion term (GGA+U method) reveal competing ground states in (111) oriented $(LaAlO_3)_M/(SrTiO_3)_N$ superlattices with n-type interfaces, ranging from spin, orbital selective, Dirac point Fermi surface to charge ordered flat band phases. The types of broken symmetry depends strongly on (i) $SrTiO_3$ quantum well thickness and (ii) $t_{2g} \rightarrow a_{1g} + e'_g$ crystal field spitting tied to in-plane strain. Symmetry breaking behavior is pronounced for the honeycomb lattice bilayer case N=2, where nearly all initial symmetries are broken (charge, spin, orbital, inversion), and we show that strain can be used to engineer between a ferromagnetic Dirac point semimetal and a charge ordered multiferroic (ferromagnetic and ferroelectric) flat band insulating phase.

PACS numbers: 73.21.Fg, 73.22.Gk, 75.70.Cn

Remarkably rich electronic behavior has been discovered at oxide interfaces ranging from two-dimensional conductivity, superconductivity and magnetism to both confinement induced and gate controlled metal-to-insulator transitions.[1] Most of the interest so far has been directed at (001) oriented interfaces as, e.g., the ones between the two band insulators $LaAlO_3$ (LAO) and $SrTiO_3$ (STO).[2–6] Recently the growth and initial characterization, including finding of a high mobility electron gas, of LAO films on STO(111) has been reported.[7] In contrast to the (001) direction where in the perovskite structure AO and BO_2 layers alternate, the (111) orientation comprises alternating stacking of AO_3 and B layers which can be highly charged: for example $(LaO_3)^{3-}/Al^{3+}$ for LAO, $(SrO_3)^{4-}/Ti^{4+}$ for STO, as illustrated in Fig. 1a. Despite the difference in stacking and charge of the individual layers, a polar discontinuity arises for both orientations, with a mismatch of exactly $0.5e$ per B cation for the n-type interfaces. For the (001) orientation this polar discontinuity is considered to be the origin of the rich spectrum of functional properties mentioned above, albeit the latter can also be influenced by defects. It is timely to investigate whether similar electronic reconstructions and exotic phases arise for the (111) orientation.

Perovskite (111) layers have distinctive real space topology: each BO_6 layer constitutes a triangular lattice where the B cations are *second* neighbors. Combining two such layers in a bilayer forms a buckled honeycomb lattice, topologically equivalent to that of graphene (Fig. 1c); three layers form the also distinctive dice lattice. The possibility for nontrivial topology of electrons hopping on a honeycomb lattice proposed by Haldane[8] has spurred model Hamiltonians studies of topologically nontrivial states for (111)-oriented perovskite superlattices,[9–11] where the focus was on the $LaNiO_3$ (LNO) e_g system confined within LAO with quadratic band touching points and a Dirac point at higher band filling.[10–12] This two-orbital honeycomb lattice is beginning to be grown and characterized.[13, 14] The corresponding three-orbital t_{2g} system is realized for STO confined in LAO, where $e/2$ charge from each n-type "interface" (IF) will force one electron into 12 Ti conduction states (2 atoms, 3 orbitals, 2 spins), initially with P321 symmetry with two generators (3-fold rotation, z mirror+$x \leftrightarrow y$, which we heuristically refer to as inversion). The result is a 12-band, potentially strongly correlated generalization of graphene subject to numerous symmetry breaking orders: charge, spin, orbital, rotation, inversion, and gauge symmetry; our methods do not address the latter.

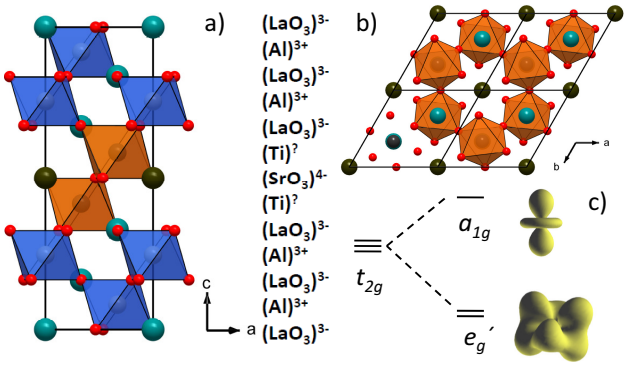

FIG. 1: a) Side view of $(LAO)_4/(STO)_2(111)$ SL with an n-type interface. b) Top view of the STO bilayer forming a buckled honeycomb lattice out of the two triangular lattices of Ti cations at each interface where Ti are second nearest neighbors. c) splitting of the t_{2g} orbitals in a_{1g} and e'_g due to trigonal symmetry.

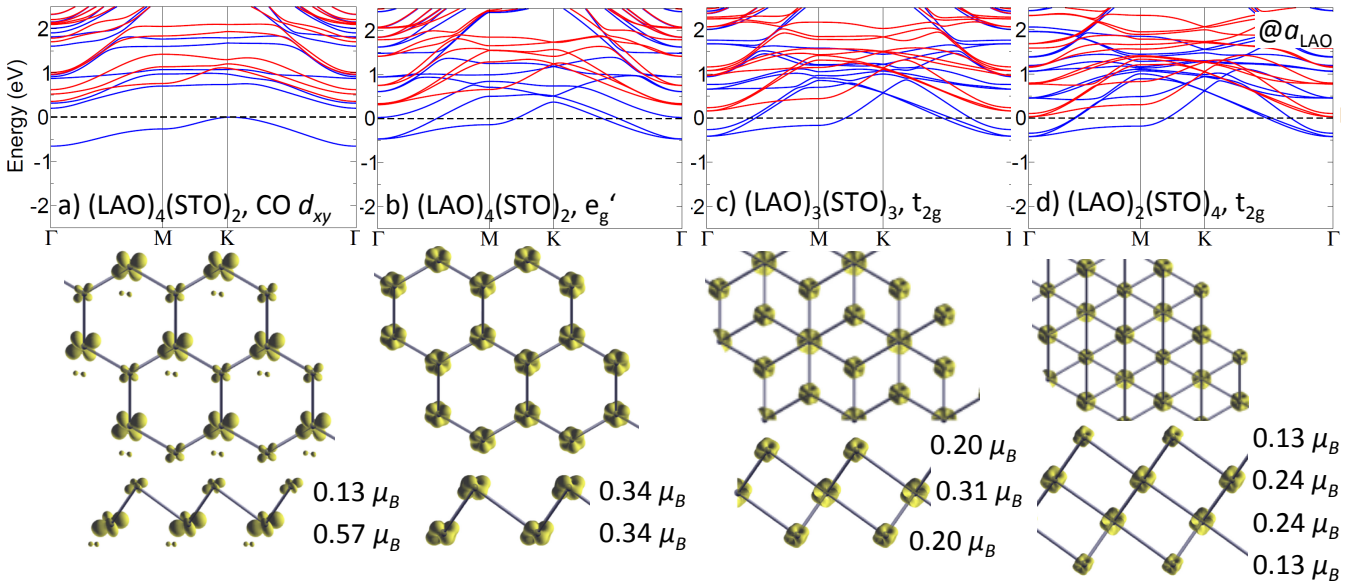

FIG. 2: Band structure and electron density distribution, integrated over occupied Ti $3d$ bands, for $(\mathrm{LAO})_N/(\mathrm{STO})_M(111)$ under compressive strain (a_{LAO}). Majority and minority bands are plotted in blue and red, respectively. a) $N = 2$ charge ordered FM insulator. Note the "d_{xy}" occupation, *i.e.* single (but unsymmetrically oriented) real t_{2g} orbital. b-d) Note also the decreasing bandwidth at Γ as well as the switching from t_{2g} ($N = 3, 4$) to e'_g orbital occupation ($N = 2$) for decreasing N_{STO}.

A key question is that of orbital polarization, which is a primary factor in magnetic, transport, and optical properties. The geometry of the 111-superlattice breaks orbital 3-fold (t_{2g}) symmetry into trigonal $t_{2g} \rightarrow e'_g + a_{1g}$ as shown schematically in Fig. 1c. For the (001) IF, previous DFT studies predicted,[15–18] and XAS data[19] demonstrated, that the t_{2g} degeneracy is lifted such that the d_{xy} orbital at the interface lies lower in energy. Including static local correlation effects within GGA+U stabilizes a charge ordered and orbitally polarized layer with alternating Ti^{3+} and Ti^{4+} in the interface layer and a d_{xy} orbital occupied at the Ti^{3+} sites.[15, 16] It will be instructive to compare this scenario with the behavior for (111) orientation.

A mathematically symmetric expression adapted to trigonal symmetry for t_{2g} orbitals is

$$|\psi_m\rangle = (\zeta_m^0|d_{xy}\rangle + \zeta_m^1|d_{yz}\rangle + \zeta_m^2|d_{xz}\rangle)/\sqrt{3},$$

where $\zeta_m = e^{2\pi i m/3}$. One issue is whether complex e'_g orbitals m=1,2 (m=0 is the a_{1g} orbital) assert themselves, inviting anomalously large response to spin-orbit coupling in t_{2g} systems,[20] or whether real combinations of the e'_g orbitals persist. Complex orbitals in the e_g bilayer have been predicted to encourage topological phases.[12] In this paper we find that trigonal level splitting, which is intimately connected to strain, affects orbital occupation which vastly influences the electronic structure in (111) oriented STO QWs.

DFT calculations have been performed on $(\mathrm{LAO})_N/(\mathrm{STO})_M(111)$ superlattices with varying thickness N, M of both constituents, using the all-electron full-potential linearized augmented plane wave (FP-LAPW) method, as implemented in the WIEN2k code [21, 22]. The LAO thickness M is always large enough to confine the carriers to STO. For the exchange-correlation potential we used the generalized gradient approximation (GGA) [23]. Static local electronic correlations were taken into account in the GGA+U method [24] with U = 5 eV, J = 0.7 eV (Ti $3d$), U = 8 eV (La $4f$). The influence of strain was investigated by choosing the lateral lattice parameter of either LAO (a_{LAO}=3.79 Å) or STO (a_{STO}=3.92 Å). Octahedral tilts and distortions were fully taken into account when relaxing atomic positions, whether constrained to P321 symmetry (3-fold rotation, plus inversion+rotation in the O site between Ti layers) or fully released to P1 symmetry.

Compressive strain (a_{LAO}) corresponding to an underlying LAO substrate. Fig. 2b-d present results for n-type (111) oriented $(\mathrm{LAO})_N/(\mathrm{STO})_M$ superlattices with different thicknesses N of the STO quantum well (QW), each of which is ferromagnetic (FM) and half metallic. For this t_{2g} bilayer we find exclusively FM states to be favored regardless of in-plane strain, restriction of symmetry, and starting configuration. Similarly, in their model studies of a e_g bilayer honeycomb lattice LNO superlattices), Rüegg *et al.*[12] found FM ordering for broad ranges of model parameters. At first sight, the difference $N \rightarrow 2-4$ in electronic structure seems minor: the flattish lower conduction band is mostly occupied, leaving

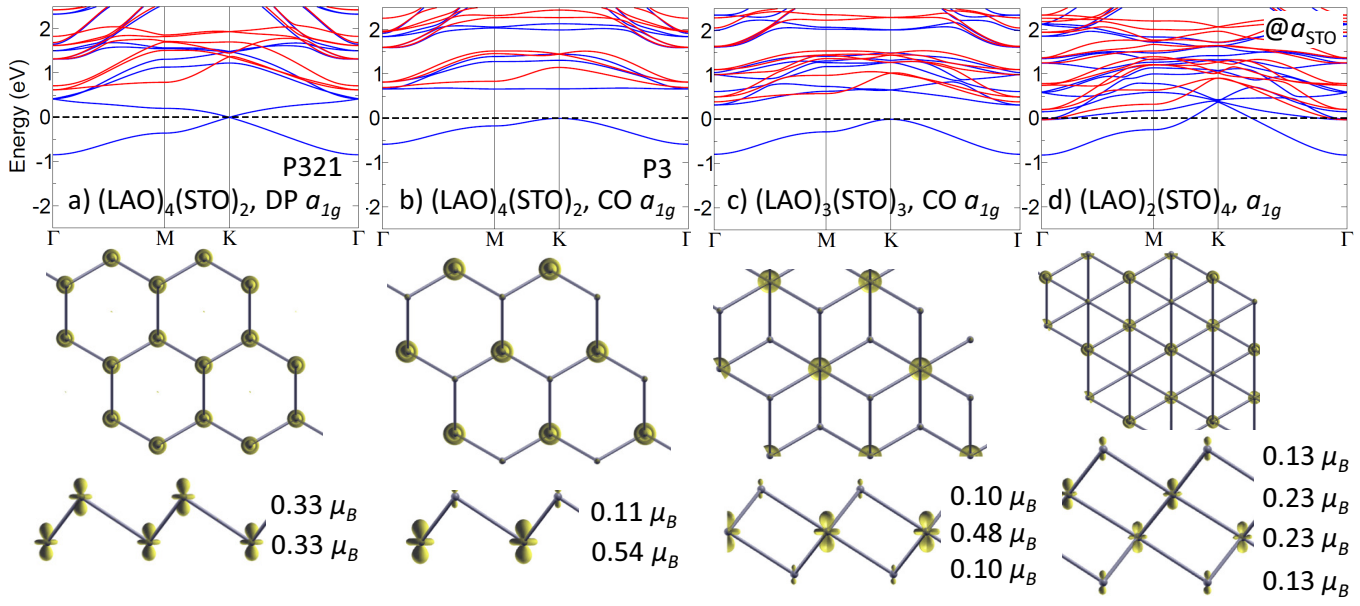

FIG. 3: As in Fig. 2, but under tensile strain ($a_{\rm STO}$). Note the a_{1g} occupation independent of N. $N = 2$: a) For the inversion symmetric interfaces the system is semimetallic with a Dirac point at K, as in graphene. b) Allowing breaking of inversion symmetry results in inequivalent interfaces, Ti^{3+}versus Ti^{4+} leading to the formation of a (111) dipole layer and insulating behavior. c-d) with increasing $N_{\rm STO}$the system switches from insulating to conducting behavior.

a hole Fermi surface (FS) surrounding the zone corner point K, with charge being balanced by one or two electron FS pockets centered at Γ. The orbital polarization, *i.e.* band character, varies strongly, however. For the thicker N=3, 4 STO QWs, t_{2g} orbitals are equally occupied, but for $N = 2$ the t_{2g}-degeneracy is lifted and the e'_g orbitals become preferentially occupied. The extra 0.5 charge from each interface is distributed preferentially towards the central layers for the thicker $N = 3$, 4 STO QWs, related to the different chemical environment of interface vs. central Ti ions. We return to Fig. 2a) below.

Tensile strain ($a_{\rm STO}$). Using the in-plane STO lattice constant, strains the LAO layer but leaves STO cubic (subject to relaxation), *reverses* the orbital polarization – a remarkably strong strain effect – and produces richer behavior: the symmetric a_{1g} orbital becomes occupied independently of the $N_{\rm STO}$ thickness, as shown in Fig. 3. Similar to the compressive case, the charge is shifted from the interface towards the central layers with increasing STO thickness. For the dice lattice (3/3) case the Ti^{3+} central layer (0.48 $\mu_{\rm B}$) is sandwiched by Ti^{4+} interface layers, a confinement effect resulting in the FM insulating ground state. An insulator-to-metal transition occurs at $N = 4$, always retaining FM order, although the exchange splitting is reduced with increasing STO QW width. For LAO layers grown on STO(111), Herranz *et al.* found a critical thickness of ∼10-12 LAO layers for the onset of conductivity, but their setup [7] is not comparable to our QW system. We can note from both Figs. 2 and 3 the proclivity of linear "Dirac" bands to occur at K, but when such points are not pinned to E_F they have no importance.

As mentioned, the case $N = 2$ is special because the Ti bilayer forms a honeycomb lattice, prompting us to study this system in more detail. The single electron can be shared equally and symmetrically by the two Ti ions, or it can tip the balance to charge order, which requires symmetry breaking from P321 to P3 or possibly P1. Each of these broad scenarios can be handled with or without other broken symmetries. We remind that we always find the spin symmetry is broken to FM order.

Compressed STO bilayer. Beginning from imposed AFM order, the bilayer with compressive strain returned to FM order (Fig. 2a), but with three momentous changes: (1) it is a *charge ordered FM insulator* Ti^{3+} ($0.57\mu_B$) and Ti^{4+} ($0.13\mu_B$), and due to broken inversion symmetry it is also ferroelectric (FE), (2) the occupied (real) orbital assumes d_{xy} orientation, and (3) the top of the gap is bounded by a remarkably flat band. This state, retaining P3 symmetry, is preferred by 25 meV/Ni over the inversion symmetric state (Fig. 2b), indicating strong competition of electronic states with distinct orbital occupation, with very different symmetries, and ungapped versus gapped.

Tensile STO bilayer. Constrained to P321 symmetry, a graphene-like Dirac point emerges at the zone corner point K that is pinned to the Fermi level and protected by the equivalence of the Ti sites, see Fig.3a. True particle-hole symmetry is restricted to relatively low energy due to coupling of the upper band to high-lying bands. The occupied bandwidth corresponds to hopping

$t_{a_{1g},a_{1g}}$=0.28 eV. Having a single electron shared symmetrically by two Ti sites is potentially unstable. Allowing breaking of this ("inversion") symmetry results again, as for compressive strain, in a CO Ti^{3+} ($0.54\mu_B$) and Ti^{4+} ($0.11\mu_B$), FM, FE, and insulating state evident from Fig. 3b. The massless-to-massive transformation of the spectrum results from the inequivalence of the Ti ions. Nearly complete charge disproportionation gives CO alternating around each honeycomb hexagon, retaining P3 symmetry although it was not imposed.

In both cases charge ordering is accompanied by formation of an electric dipole in the bilayer as well as Ti-O bond alternation: in the latter tensile case the Ti-Ti interlayer distance is 2.1Å, and Ti^{4+}-O (Ti^{3+}-O) distance of 1.90Å (1.96Å), respectively (being 1.93Å in the symmetric case). The orbital polarization, pure a_{1g} occupation, is distinct to the CO state for compressive strain, which has occupation of a single real t_{2g}-like orbital, which is a visibly tilted d_{xy}orbital. The complex occupied orbitals that arise in QWs of $SrVO_3$[20] and VO_2[25] are not found in the present system.

The occupied bandwidths and shapes are very similar for the CO states of the two strains, and in each case the gap of ∼0.8 eV leads to a higher-lying flat band, which forms the top of the gap in the tensile case into which doped electrons would go. Nearly flat bands have been obtained in a variety of contexts: from a d-p_x-p_y square lattice model [26] and from a p_x,p_y honeycomb lattice model [27]; Xiao *et al.*[9] and Fiete and collaborators[12, 28] found that perfectly flat bands emerge in an e_g bilayer model, and Rüegg *et al.* demonstrated [12] that they arise from strictly localized eigenstates with symmetric orbital ordering; several others have been discovered and studied.[29–34] The flat band we find occurs only for the CO states (which are the ground states) that involve separate a_{1g} and d_{xy} orbital occupation. Its origin therefore is not as straightforward as for the above mentioned models.

The difference in on-site 3d energies becomes essential for modeling the splitting of the Dirac pair into the gapped bands. This difference in Ti^{4+} and Ti^{3+} 3d energies will be similar to the 2p core level difference, which at 1.7 eV is twice the occupied bandwidth of the Dirac band structure. Focusing on the majority (blue) bands of the CO state, a regularity can be seen: there is parallel pair of bands of the same shape as the occupied band, but lying 1.3 eV higher, which is the pair of Ti^{3+} e'_g bands. Mirroring the flat band and again 1.3 eV higher are two more (no longer precisely) flat bands; these are the Ti^{4+} a_{1g} and e'_g bands. The driving force of this charge order is on-site correlation, whose primary effect is to induce integer orbital occupations, *i.e.* a Mott insulating state. In this case, two half-filled sites (spin-orbitals) convert to one filled, the other empty. This tendency may be aided by intersite Coulomb repulsion, and certainly by oxygen relaxation accompanying the charge order.

Bands on the same graphene lattice, displaying the topology that we find for the Dirac bilayer, have been related to topological character.[9–11] Typically topological phases are protected by time reversal symmetry coupled with additional symmetries. Fu [35] and others [36, 37] have noted that SOC is not required, demonstrating topological band insulators can also be protected by crystalline symmetry. In all of the present cases FM order breaks time reversal symmetry, so topological character becomes progressively less likely.

The various phases we have discussed have broken all possible symmetries except 3-fold rotation with a single Ti^{3+}-Ti^{4+} distance. Specifically, no Ti^{3+}-Ti^{4+} nor $Ti^{3.5+}$-$Ti^{3.5+}$, dimerization has been obtained. The latter could promote a triangular lattice version of the dimer Mott insulator (DMI),[38, 39] a phase that is is known to compete with charge ordering and loses in this bilayer. The DMI ground state appears to account for the metal-insulator transition in quasi-2D organic crystals[38] and has been suggested to arise in a digital oxide nanostructures,[40] and a trimer Mott insulating phase accounts for MIT in the insulating 2D nickelate $La_4Ni_3O_8$ with average $Ni^{4/3+}$ charge state.[41]

To summarize, unexpected richness has been uncovered in (111)-oriented STO/LAO heterostructures, where carriers must reside in Ti t_{2g} states. The competing ground states are, in contrast to (001) orientation, ferromagnetic, with orbital and charge order determined by strain-controlled crystal field splitting $t_{2g} \rightarrow a_{1g} + e'_g$ that promotes strain engineering of properties. For the system under tensile strain, a graphene-like Dirac point degeneracy survives as long as inversion symmetry of the bilayer is preserved. Allowing breaking of this symmetry, charge ordering with a flat conduction band and multiferroic properties results, but with orbital polarization dependent on strain. Melting of the CO phase as temperature is raised, where several symmetries (and conductivity) are restored, should reveal very rich behavior.

R.P. acknowledges discussions with M. Rozenberg. R.P. and D. D. acknowledge financial support through the DFG SFB/TR80 and grant *h0721* for computational time at the Leibniz Rechenzentrum. W. E. P. was supported by U.S. Department of Energy Grant No. DE-FG02-04ER46111.

* Electronic address: rossitzap@lmu.de

[1] H. Y. Hwang, Y. Iwasa, M. Kawasaki, B. Keimer, N. Nagaosa, and Y. Tokura, Nat. Mater. **11**, 103 (2012).
[2] M. Huijben, A. Brinkman, G. Koster, G. Rijnders, H. Hilgenkamp, and D. A. Blank Adv. Mater. **21**, 1665 (2009).
[3] J. Mannhart and D. G. Schlom, Science **327**, 1607 (2010).
[4] R. Pentcheva and W. E. Pickett, J. Phys.: Condens. Matter **32**, 043001 (2010).

[5] P. Zubko, S. Gariglio, M. Gabay, P. Ghosez, and J.-M. Triscone, Annu. Rev. Condens. Matter Phys. **2**, 141 (2011).

[6] R. Pentcheva, R. Arras, K. Otte, V. G. Ruiz, and W. E. Pickett, Phil. Trans. R. Soc. A **370**, 4904 (2012).

[7] G. Herranz, F. Sanchez, N. Dix, M. Scigaj, and J. Fontcuberta, Scientific Reports (Nature group) **2**, 758 (2012).

[8] F. D. M. Haldane, Phys. Rev. Lett. **61**, 2015 (1988).

[9] D. Xiao, W. Zhu, Y. Ran, N. Nagaosa, and S. Okamoto, Nature Commun. **2**, 596 (2011).

[10] A. Rüegg and G. A. Fiete, Phys. Rev. B **84**, 201103 (2011).

[11] K.-Y. Yang, W. Zhu, D. Xiao, S. Okamoto, Z. Wang, and Y. Ran, Phys. Rev. B **84**, 201104(R) (2011).

[12] A. Rüegg, C. Mitra, A. A. Demkov, and G. A. Fiete, Phys. Rev. B **85**, 245131 (2012).

[13] M. Gilbert, P. Zubko, R. Scherwitzl, and J.-M. Triscone, Nat. Mater. **11**, 195 (2012).

[14] S. Middey *et al.*, Appl. Phys. Lett. **101**, 261602 (2012).

[15] R. Pentcheva and W. E. Pickett, Phys. Rev. B **74**, 035112 (2006).

[16] R. Pentcheva and W. E. Pickett, Phys. Rev. B **78**, 205106 (2008).

[17] Z. Zhong and P. J. Kelly, Eur. Phys. Lett. **84**, 27001, (2008).

[18] Z. S. Popovic, S. Satpathy, and R. M. Martin, Phys. Rev. Lett. **101**, 256801 (2008).

[19] M. Salluzzo *et al.*, Phys. Rev. Lett. **102**, 166804 (2009).

[20] V. Pardo and W. E. Pickett, Phys. Rev. B **81**, 245117 (2010).

[21] K. Schwarz and P. Blaha, Comp. Mat. Sci. **28**, 259 (2003).

[22] P. Blaha, K. Schwarz, G. K. H. Madsen, D. Kvasnicka, and J. Luitz, *WIEN2k, An Augmented Plane Wave Plus Local Orbitals Program for Calculating Crystal Properties*, ISBN 3-9501031-1-2 (Vienna University of Technology, Vienna, Austria, 2001).

[23] J. P. Perdew, K. Burke, and M. Ernzerhof, Phys. Rev. Lett. **77**, 3865 (1996).

[24] V. I. Anisimov, J. Zaanen, and O. K. Andersen, (1993).

[25] V. Pardo and W. E. Pickett, Phys. Rev. B **81**, 035111 (2010).

[26] K. Sun, Z. Gu, H. Katsura, and S. Das Sarma, Phys. Rev. Lett. **106**, 236803 (2011).

[27] C. Wu, D. Bergman, L. Balents, and S. Das Sarma, Phys. Rev. Lett. **99**, 070401 (2007).

[28] X. Hu, A. Rüegg, and G. A. Fiete, Phys. Rev. B **86**, 235141 (2012).

[29] D. L. Bergman, C. Wu, and L. Balents, Phys. Rev. B 78, 125104 (2008).

[30] C. Weeks and M. Franz, Phys. Rev. B **85**, 041104 (2012).

[31] F. Wang and Y. Ran, Phys. Rev. B **84**, 241103(R) (2011).

[32] J.-M. Hou, Commun. Theor. Phys. **52**, 247 (2009).

[33] D. Green, L. Santos, and C. Chamon, Phys. Rev. B **82**, 075104 (2010).

[34] H. Katsura, I. Maruyama, A. Tanaka, and H. Tasaki, EPL (Europhysics Letters) **91**, 57007 (2010).

[35] L. Fu, Phys. Rev. Lett. **106**, 106802 (2011).

[36] M. Kargarian and G. A. Fiete, arXiv:1212:4162.

[37] R.-J. Slager *et al.*, Nat. Phys. **9**, 98 (2013).

[38] H. Kino and H. Fukuyama, J. Phys. Soc. Japan **64**, 1877 (1995).

[39] H. Seo, J. Merino, H. Yoshioka, and M. Ogata, J. Phys. Soc. Japan **75**, 051009 (2006).

[40] R. Chen, S.-B. Lee, and L. Balents, arXiv:1301.4222.

[41] V. Pardo and W. E. Pickett, Phys. Rev. Lett. **105**, 266402 (2010).